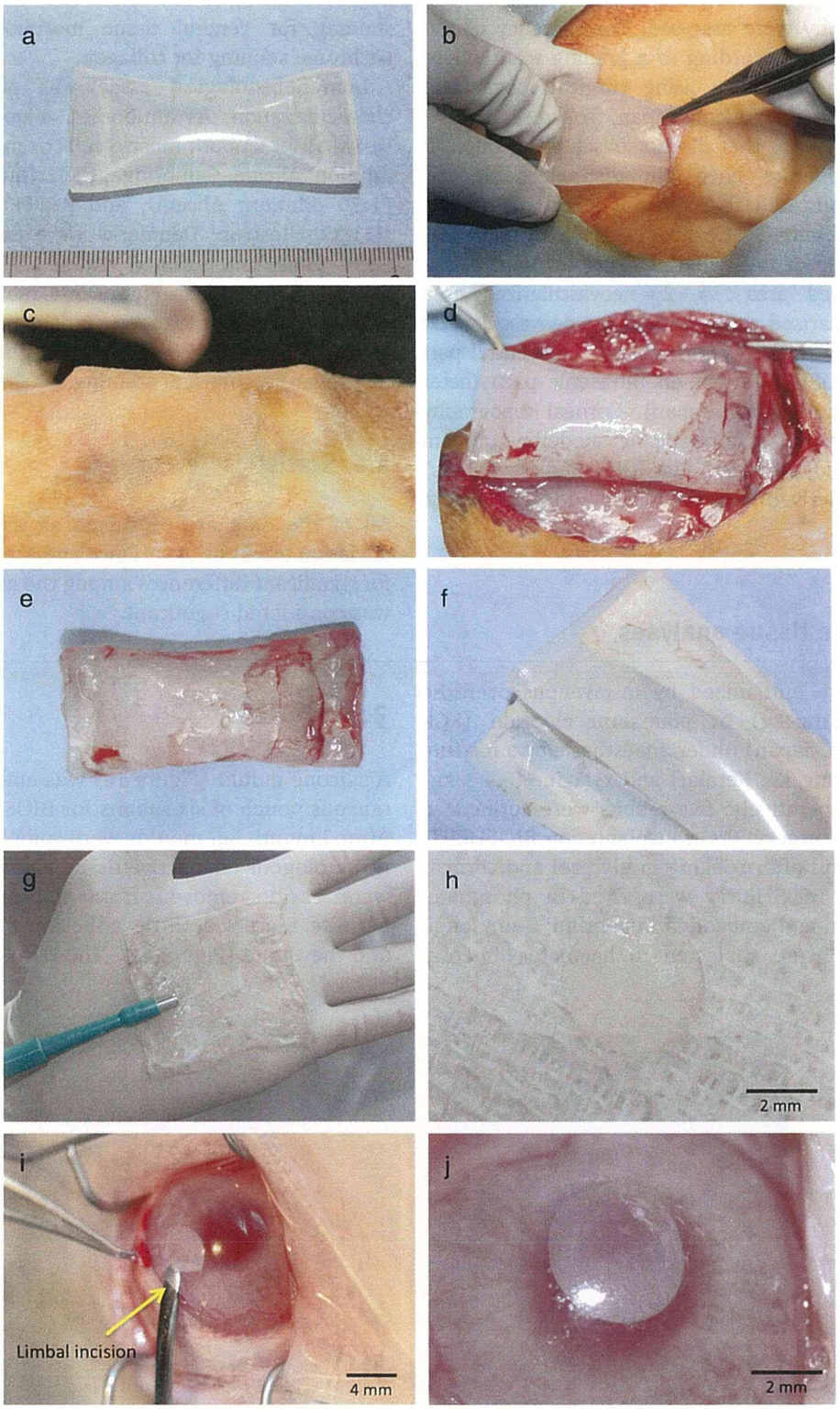

Figure 1. Preparation and implantation of BIOSHEET. (a) Silicone mould for BIOSHEET preparation. The mould at (b) and after (c) placing into the subcutaneous pouch; (d) The mould encapsulated completely with BIOSHEET tissue after 1 month of implantation; (e) BIOSHEET-covered mould after trimming to remove fragile and redundant tissue; (f,g) BIOSHEET preserved by soaking in sterile pure glycerol and submerged in physiological saline; (h) trephined BIOSHEET (4 mm in diameter); (i) implantation into stromal pocket of rabbit cornea; (j) immediately after implantation

($n = 4$). The incision was closed with one suture using 10–0 nylon, which was removed 2 weeks after surgery. After surgery, 5 mg/kg systemic enrofloxacin (Baytril injectable; Bayer) was administered daily for the first week. No immunosuppressive drugs were used.

2.4. Clinical test

Follow-up evaluations were performed daily on each rabbit for 7 days after surgery and then weekly. Corneal opacity grade, vascularization, corneal thickness and

corneal topography were assessed. Transparency of the cornea was assessed according to a grading scale where 0 indicated transparent by using surgical microscope (×10 ~ 20, OPMI pico; Alcon Japan, Tokyo, Japan), 1 indicated a slight haze that did not obscure the pupil, 2 indicated a moderate haze but distinguishable iris vessels and 3 indicated that the pupil and iris vessels were totally obscured. Corneal vascularization was graded on a scale of 0–4 where 0 = no vascularization, 1 = neovascularized area < ¼, 2 = neovascularized area ½, 3 = neovascularized area < ¾ and 4 = neovascularized area > ¾. Corneal thickness was measured at central part of implanted BIOSHEET with an ultrasonic pachymeter (AL-3000; Tomey, Nagoya, Japan). Corneal topography was measured using a topographic modelling system (TMS-4 Advanced; Tomey). Flat (Kf) and steep (Ks) meridians were derived from the measured topography of each cornea.

2.5. Qualitative tissue analyses

Two rabbits were euthanized by intravenous overdose (more than 75 mg/kg) of potassium chloride (KCl; Nichiiko, Toyama, Japan) under anaesthesia by a mixture of ketamine (50 mg/kg, Ketalar) and xylazine (5 mg/kg) at 4 weeks postoperatively; five rabbits were euthanized at 8 weeks after surgery. Pre-transplantation BIOSHEETs ($n = 2$) before and after soaking in glycerol and corneas implanted with BIOSHEETs were fixed in phosphate-buffered formalin and embedded in paraffin; 5-μm longitudinal sections were subjected to haematoxylin-eosin staining for general tissue morphology and Masson trichrome staining for collagen.

Immunohistological assay was performed for cell characterization. As antibodies, α-smooth muscle actin (α-SMA) for smooth muscle cells or myofibroblasts (1:50 dilution; Abcam, Cambridge, UK), vimentin for fibroblasts (1:50 dilution; Abcam), and RAM11 for macrophages (DAKO, Glostrup, Denmark) were used. After washing with phosphate-buffered saline (PBS), slides were incubated with Alexa Fluor®594 rabbit anti-mouse IgG antibody (1:200; Invitrogen, Carlsbad, CA, USA) and then incubated with 4′,6-diamidino-2-phenylindole (DAPI; Invitrogen) for nuclear staining.

2.6. Statistics

All of the data are expressed as the mean ± standard deviation. Analysis of variance and *t*-test were used to test for significant differences among the groups, and $p < 0.05$ was considered significant.

3. Results

A silicone mould (Figure 1a) was embedded in a subcutaneous pouch of six rabbits for BIOSHEET preparation. After 1 month, all moulds were completely encapsulated by autologous connective tissue membrane. The moulds were easily removed from the membranous tissue because there was little adhesion between the mould and the tissue (Figure 1f). The tissue obtained (i.e. the

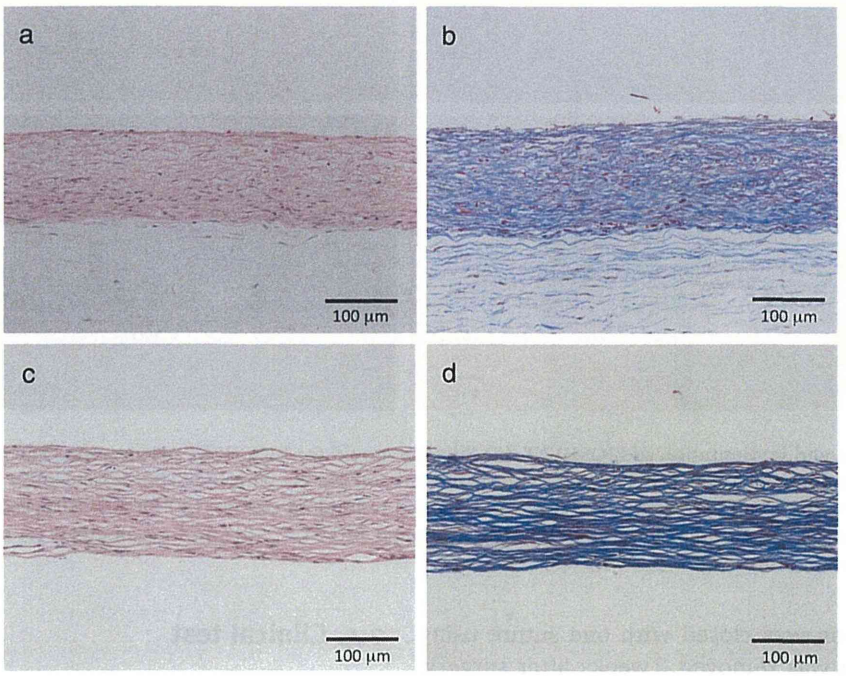

Figure 2. Haematoxylin and eosin section of BIOSHEETs before (a) and after (c) preservation in glycerine and submerged in physiological saline, and Masson's trichrome section of BIOSHEETs before (b) and after (d) preservation in glycerine and submerged in physiological saline

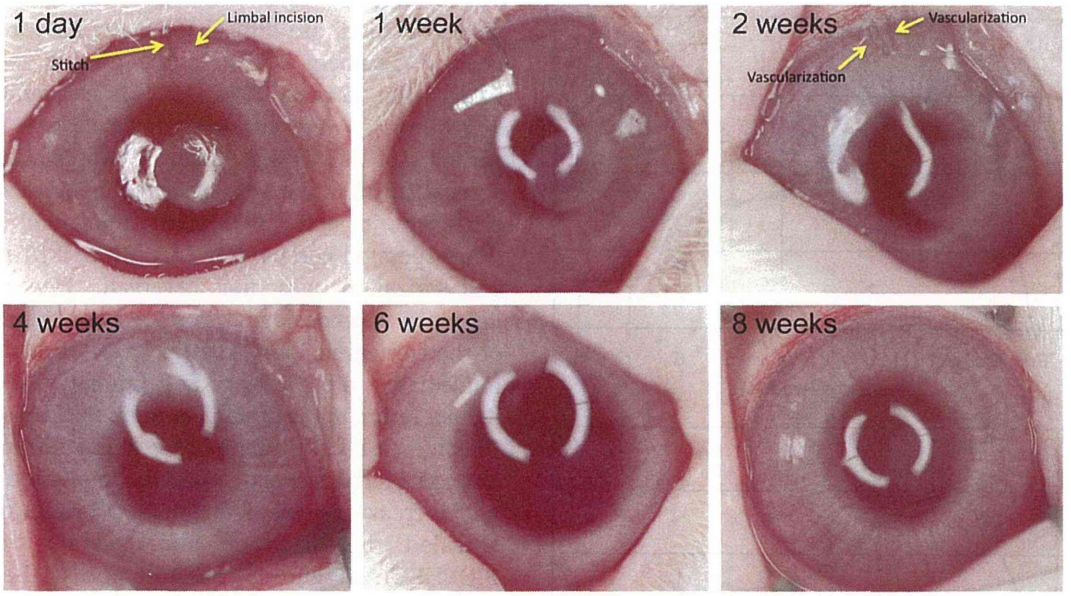

Figure 3. Postoperative observation of BIOSHEET implanted into rabbit corneal stroma

BIOSHEETs) comprised thin sheets with a smooth flat surface (6 × 6.5 cm, 131.0 ± 14.0 μm thick, Figure 1g). The success rate of BIOSHEET preparation was, therefore, 100%. However, it was opaque both before and after glycerol preservation (Figure 1h) with random orientation of the collagen fibres (Figure 2b,d). All cells in the BIOSHEET died after the it was immersed into glycerol for 1 week although many cell nuclei remained (Figure 2c).

All animals survived without infections or other complications during the follow-up period. Neo-vascularization, corneal thickness, corneal refractive power and histology were evaluated to investigate the possibility of the BIOSHEET as a corneal stromal substitution material. Slight corneal neovascularization that reached the corneal incision was noted up to 2 weeks postoperatively (Figure 3). The average corneal vascularized scores of BIOSHEET implanted corneas were 0.7 ± 0.5 at 1 week and 0.1 ± 0.4 at 2 weeks, which were almost same of those of sham-operated corneas (0.75 ± 1.0 at 1 week, 0.5 ± 1.0 at 2 weeks). At 4 weeks after implantation or sham operation all corneas had no neovascularization (scores 0). In addition, there was no inflammation or signs of rejection during implantation. Immediately after implantation, all BIOSHEET disks were opaque (Figure 1h). However, interestingly, each BIOSHEET became transparent over time in all rabbits (Figure 3). The transparency scores for the cornea after 4 weeks were significantly lower (1.7 ± 1.0 at 4 weeks and 0.6 ± 0.6 at 8 weeks) than those obtained immediately after implantation (3, $p < 0.05$) (Figure 4a). The transparency of the cornea increased progressively with time of implantation.

The total thickness of the cornea was 726.1 ± 131.0 μm immediately after implantation and almost the same even at 2 weeks after implantation (Figure 4b). The thickness was significantly greater than the pre-implantation thickness (364 ± 21.0 μm). Thickness markedly decreased in the first 4 weeks (493.0 ± 80.0 μm) and then remained stable until 8 weeks (447.0 ± 46.0 μm).

The increased postoperative corneal refractive power was attributed to the implanted BIOSHEETs and increased corneal thickness. After implantation, high refractive power (Figure 4c) and rough corneal topography remained (Figure 5).

The arrangement and orientation of the collagen lamellae of BIOSHEETs were heterogeneous at 4 weeks postoperatively, but they tended to take on a homogeneous character similar to that of the native corneal stroma at 8 weeks postoperatively (Figure 6). The boundaries of the BIOSHEETs were well defined at 4 weeks but became indistinct at 8 weeks. At 8 weeks after implantation fibroblast-like cells infiltrated into the implanted BIOSHEETs (Figure 7a), but there were no α-SMA positive cells (Figure 7b) or inflammatory cells (Figure 7c).

4. Discussion

The cornea is responsible for transmission and refraction of the light to the retina and for maintaining the shape of the eye. The cornea is an avascular and transparent tissue composed of three layers: the epithelium, stroma and endothelium. The extracellular matrix of the corneal stroma consists primarily of collagen type I with a lower amount of collagen type IV and proteoglycans (Knupp *et al.*, 2009; Hassell and Birk, 2010). Therefore, collagenous biomaterials such as collagen gels, and acellular porcine corneas are widely used as potential corneal substitutes (Liu *et al.*, 2007; Fagerholm *et al.*, 2009, 2010; Merrett *et al.*, 2009; Duncan *et al.*, 2010; Tanaka *et al.*, 2011; Xiao *et al.*, 2011; Yoeruek *et al.*, 2011). As alternative approach, autogenic transplantation of collagen-rich tissues such as ligaments,

DOI: 10.1002/term

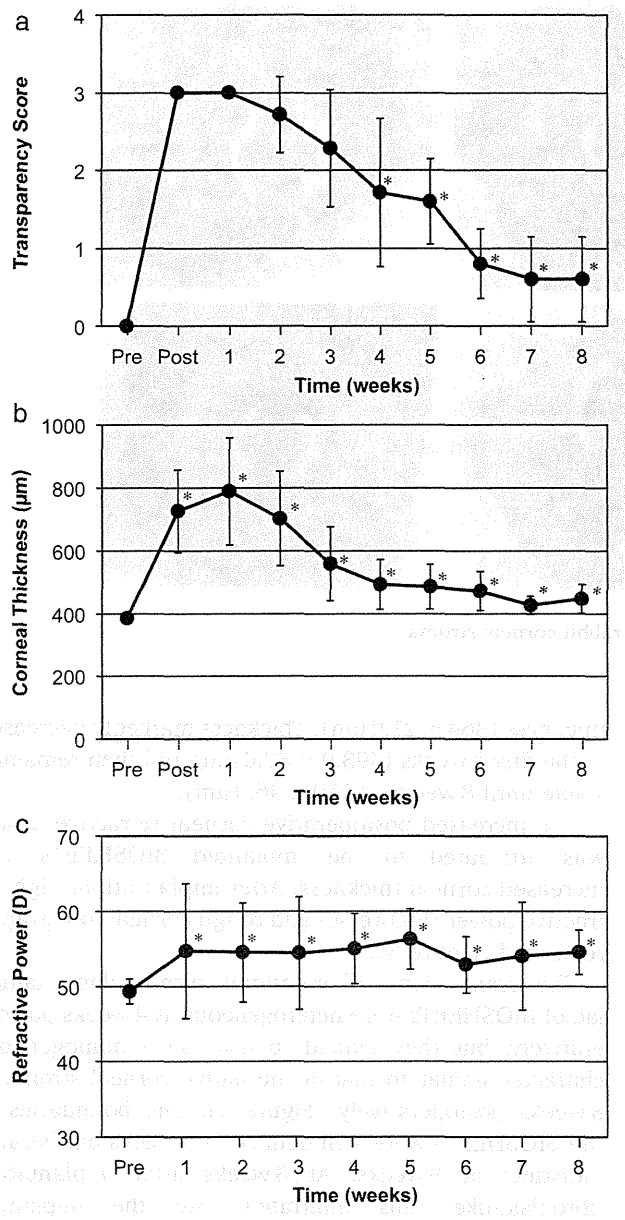

Figure 4. (a) Mean values for corneal transparency. The corneas implanted with the BIOSHEET became hazy immediately after transplantation, but transparency was gradually restored. (b) Change in corneal thickness following implantation of BIOSHEETs into rabbit cornea. (c) Refractive power change following implantation of BIOSHEETs into rabbit cornea. Significant increase from preoperative values (*, $P < 0.05$)

tendons, and skin have been widely applied for the replacement of damaged tissue (Jackson and Simon, 2002; Antonogiannakis *et al.*, 2005; de Vries Reilingh *et al.*, 2007; Carey *et al.*, 2009). However, there is no adequate autogenic tissue source (i.e. a tissue with high transparency and high mechanical strength) for substitution of the corneal stroma. Therefore, the primary goal of this study was to prepare collagenous membranes as BIOSHEETs for corneal stromal substitution. We evaluated the biocompatibility and transparency of BIOSHEETs transplanted into rabbit corneal stroma.

Biocompatibility factors, including cell compatibility, lack of immunogenicity, lack of toxicity and resistance to biodegradation, are critical for materials for tissue engineering (Feinberg 2012). In the present study, neovascularization, corneal thickness, corneal refractive power and histology were evaluated to investigate the biocompatibility of BIOSHEETs. Slight neovascularization of the corneal incision site was observed up to 2 weeks postoperatively in both BIOSHEETs implanted cornea and sham-operated cornea; however, BIOSHEET-induced neovascularization was not observed. Hence, neovascularization was considered to represent the wound healing of the corneal incision. The thickness of cornea increased immediately after surgery and gradually decreased; but did not return to the preimplantation thickness (Figure 4B). The increased postoperative corneal refractive powers are considered to result from the implanted BIOSHEETs and increased corneal thickness. Corneal topographies revealed the existence and location of implanted BIOSHEETs (Figure 5). Histologically, the BIOSHEET remained between stromal layers. The implanted BIOSHEET was infiltrated with corneal fibroblasts but not inflammatory cells. These results indicate that the BIOSHEET was well tolerated without inflammation, degradation or any signs of rejection, even though the implantation was allogeneic. Therefore, BIOSHEETs prepared using our technique appear to have excellent biocompatibility for corneal tissue.

This finding was expected based on our previous study of the implantation of cardiovascular tissues prepared similarly (Nakayama *et al.*, 2004; Hayashida *et al.*, 2007; Watanabe *et al.*, 2011; Yamanami *et al.*, 2010). BIOSHEETs mainly consist of collagen type I, which is the main biochemical component of the skin and corneal stroma (Knupp *et al.*, 2009; Hassell and Birk, 2010; Robert *et al.*, 2001). This similarity in composition between the native cornea and BIOSHEETs may underlie the high biocompatibility of BIOSHEETs implanted into the corneal stroma. The implanted BIOSHEETs were preserved in sterile pure glycerol, which is a simple, effective and economical preservation medium (King *et al.*, 1962; Sharma *et al.*, 2001). Glycerol-preserved tissue lacks antigenicity, which thus prevents graft rejection and obviates long-term immunosuppressive treatment (Chen *et al.*, 2010). Preservation in glycerol may have thus facilitated the engraftment of allogeneic BIOSHEETs into the rabbit cornea.

In this study, the original BIOSHEETs were opaque and obscured the pupil until several weeks after implantation; however, corneal transparency recovered progressively. The transparency of the normal cornea mainly depends on the architecture of the corneal stroma. Uniform collagen fibril diameter, uniform inter-fibrillar distance and orthogonal alignment of collagen fibres are necessary for corneal transparency (Knupp *et al.*, 2009; Hassell and Birk, 2010). Loss of transparency in the wounded cornea is caused by increased corneal thickness and increased diameter of collagen fibrils as well as poor fibrillar organization in the regenerated stroma (Quantock *et al.*, 1994). In this study, the corneas implanted with BIOSHEETs were thick and hazy immediately after implantation.

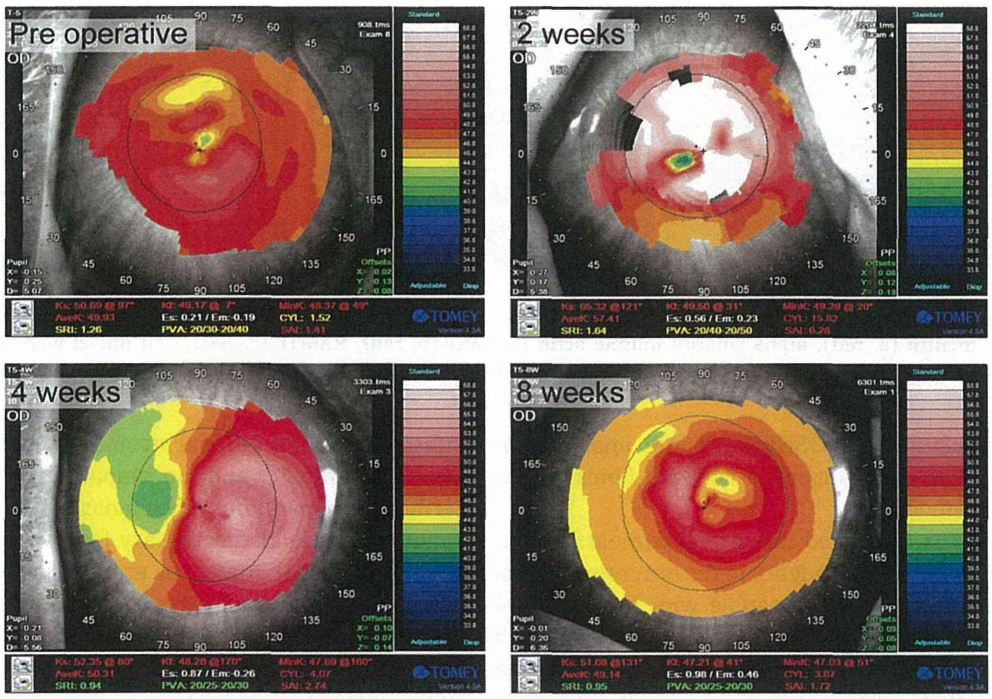

Figure 5. Change in corneal topography following implantation of BIOSHEETs into rabbit cornea

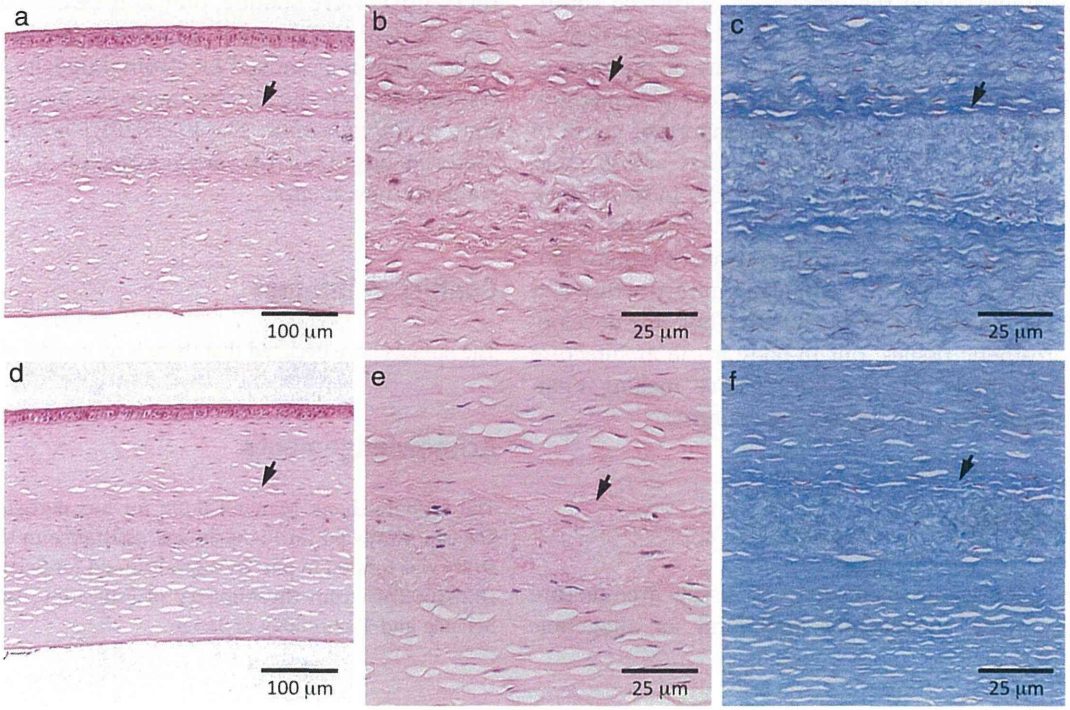

Figure 6. Histological section of rabbit corneas implanted with BIOSHEETs at 4 weeks (a–c) and 8 weeks postoperatively (d–f). Black arrows indicate the anterior surface of the implanted BIOSHEET. (a,d) Low-magnification images and (b,e) high-magnification images of haematoxylin and eosin-stained sections. (c,f) High-magnification images of Masson trichrome-stained sections

However, at 4 weeks postoperatively, the corneal thickness and the transparency score had decreased. The increase in corneal thickness and corneal opacity observed immediately after implantation may have been caused by the swelling of the BIOSHEETs, and the subsequent decrease in corneal thickness and recovery of transparency may be attributed to dehydration of the BIOSHEETs. At 8 weeks postoperatively, the transparency score had improved ($p = 0.04$), the corneal thickness had not changed and the histological arrangement and orientation of collagen lamellae of implanted BIOSHEETs became homogeneous relative to the sheets observed at 4 weeks. These results suggest that recovery of corneal transparency from 4 weeks to 8 weeks results from structural changes such as remodelling of the BIOSHEETs without degradation, thereby altering the light-scattering properties. The

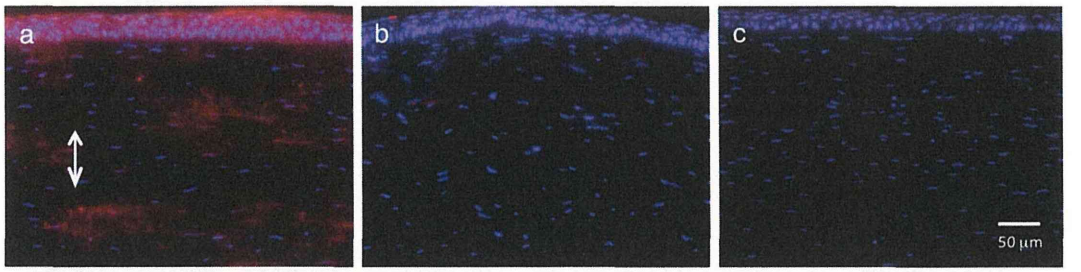

Figure 7. Immunohistological section of rabbit corneas implanted with BIOSHEETs at 8 weeks. Fluorescent microscopic images stained with vimentin (a, red), alpha smooth muscle actin (α-SMA) (b, red), RAM11 (c, red). Cell nuclei were stained with 4′,6-diamidino-2-phenylindole (DAPI, blue). White double arrow indicates the region of BIOSHEET implantation

histological structure of BIOSHEETs before implantation showed a lamellar arrangement of collagen fibres, which may facilitate remodelling.

The BIOSHEETs implanted into rabbit corneas showed high biocompatibility and tendency to restore corneal transparency. These results are compatible with the results of other studies of biosynthetic corneal implant materials such as recombinant human collagen hydrogels, decellularized corneas and rabbit dermis (Liu *et al.*, 2007; Fagerholm *et al.*, 2009; Merrett *et al.*, 2009; Duncan *et al.*, 2010; Tanaka *et al.*, 2011). Recent developments in tissue engineering technology and the production of corneal substitutes may be used to address the worldwide shortage of acceptable donor corneas. However, many of the present approaches require costly equipment and complex methodology. Globally, corneal opacity is an important cause of blindness or severe visual impairment that affects more than 10 million people, most of whom live in developing countries (Whitcher *et al.*, 2001, 2002; Schwartz *et al.*, 1997). Corneal transplantation in these areas has many limitations, including a lack of eye banking infrastructure and excessive cost (Feilmeier *et al.*, 2010). Thus, for development of prosthetic tissues, our in-body tissue architecture technology is simple, safe and cost-effective, making it particularly advantageous in developing countries.

5. Conclusion

BIOSHEETs fabricated using in-body tissue architecture technology were successfully implanted as allogeneic substitutes in the corneal stroma in a rabbit model with biological stability and biocompatibility. However, long-term biocompatibility, mechanical strength and graft innervation are also necessary for an ideal corneal scaffold. Mechanical properties are also important for tissue engineering materials. Studies to evaluate the mechanical properties of BIOSHEETs are therefore in progress. Further studies will address the long-term biocompatibility, ultrastructural changes, strength, reinnervation, and functionality of implanted BIOSHEETs in both normal and damaged cornea. Although the original BIOSHEETs were opaque, they may be considered a practical corneal replacement, especially in treatment for visual impairment caused by stromal opacity, because the transparency of the cornea increased progressively with time of implantation. The BIOSHEET is the first corneal material based on the novel concept of conversion to transparency *in situ*.

Conflict of interest

The authors have declared that there is no conflict of interest.

Acknowledgements

The authors thank Manami Sone for her participation and Dr Takeshi Moriwaki for his technical assistance in this study. This study was funded in part by a grant-in-aid for Scientific Research (B23360374) from the Ministry of Education, Culture, Sports, Science and Technology of Japan.

References

Antonogiannakis E, Yiannakopoulos CK, Hiotis I, *et al.* 2005; Arthroscopic anterior cruciate ligament reconstruction using quadriceps tendon autograft and bioabsorbable cross-pin fixation. *Arthroscopy* **21**: 894.e1–e5.

Bray LJ, George KA, Ainscough SL, *et al.* 2011; Human corneal epithelial equivalents constructed on *Bombyx mori* silk fibroin membranes. *Biomaterials* **32**: 5086–5091.

Builles N, Justin V, André V, *et al.* 2007; Reconstructed corneas: effect of three-dimensional culture, epithelium, and tetracycline hydrochloride on newly synthesized extracellular matrix. *Cornea* **26**: 1239–1248.

Carey JL, Dunn WR, Dahm DL, *et al.* 2009; A systematic review of anterior cruciate ligament reconstruction with autograft compared with allograft. *J Bone Joint Surg Am* **91**: 2242–2250.

Chen J, Li Q, Xu J, *et al.* 2005; Study on biocompatibility of complexes of collagen–chitosan–sodium hyaluronate and cornea. *Artif Organs* **29**: 104–113.

Chen W, Lin Y, Zhang X, *et al.* 2010; Comparison of fresh corneal tissue versus glycerin-cryopreserved corneal tissue in deep anterior lamellar keratoplasty. *Invest Ophthalmol Vis Sci* **51**: 775–781.

Chong EM, Dana MR. 2008; Graft failure IV. Immunologic mechanisms of corneal transplant rejection. *Int Ophthalmol* **28**: 209–222.

Crawford GJ, Constable IJ, Chirila TV, *et al.* 1993; Vijayasekaran S, Thompson DE. Tissue interaction with hydrogel sponges implanted in the rabbit cornea. *Cornea* **12**: 348–357.

Doane MG, Dohlman CH, Bearse G. 1996; Fabrication of a keratoprosthesis. *Cornea* **15**: 179–184.

Duncan TJ, Tanaka Y, Shi D, *et al.* 2010; Flow-manipulated, crosslinked collagen gels for use as corneal equivalents. *Biomaterials* **31**: 8996–9005.

Fagerholm P, Lagali NS, Carlsson DJ, *et al.* 2009; Corneal regeneration following implantation of a biomimetic tissue-engineered substitute. *Clin Transl Sci* **2**: 162–164.

Fagerholm P, Lagali NS, Merrett K, *et al.* 2010; A biosynthetic alternative to human donor tissue for inducing corneal regeneration: 24-month follow-up of a phase 1 clinical study. *Sci Transl Med* **2**: 46–61.

Feinberg AW. 2012; Engineered tissue grafts: opportunities and challenges in regenerative medicine. *WIREs Syst Biol Med* **4**: 207–220.

Feilmeier MR, Tabin GC, Williams L, *et al.* 2010; The use of glycerol-preserved corneas in the developing world. *Middle East Afr J Ophthalmol* **17**: 38–43.

Hassell JR, Birk DE. 2010; The molecular basis of corneal transparency. *Exp Eye Res* **91**: 326–335.

Hayashida K, Kanda K, Yaku H, *et al.* 2007; Development of an *in vivo* tissue-engineered, autologous heart valve (the biovalve): preparation of a prototype model. *J Thorac Cardiovasc Surg* **134**: 152–159.

Jackson DW, Simon TM. 2002; Donor cell survival and repopulation after intra-articular transplantation of tendon and ligament allografts. *Microsc Res Tech* **58**: 25–33.

King JH Jr, McTigeu JW, Meryman HT. 1962; A simple method of preservation of corneas for lamellar keratoplasty. *Am J Ophthalmol* **53**: 445–449.

Knupp C, Pinali C, Lewis PN, *et al.* 2009; The architecture of the cornea and structural basis of its transparency. *Adv Protein Chem Struct Biol* **78**: 25–49.

Lee SD, Hsiue GH, Kao CY, *et al.* 1996; Artificial cornea: surface modification of silicone rubber membrane by graft polymerization of pHEMA via glow discharge. *Biomaterials* **17**: 587–595.

Li J, Shi S, Zhang X, *et al.* 2012; Comparison of different methods of glycerol preservation for deep anterior lamellar keratoplasty eligible corneas. *Invest Ophthalmol Vis Sci* **53**: 5675–5685.

Liu L, Kuffová L, Griffith M, 2007; Immunological responses in mice to full-thickness corneal grafts engineered from porcine collagen. *Biomaterials* **28**: 3807–3814.

Merrett K, Liu W, Mitra D, *et al.* 2009; Synthetic neoglycopolymer-recombinant human collagen hybrids as biomimetic crosslinking agents in corneal tissue engineering. *Biomaterials* **30**: 5403–5408.

Nakayama Y, Ishibashi-Ueda H, Takamizawa K. 2004; *In vivo* tissue-engineered small-caliber arterial graft prosthesis consisting of autologous tissue (biotube). *Cell Transplant* **13**: 439–449.

National Institutes of Health. 1996; Guide for the Care and Use of Laboratory Animals. NIH Publication No. 85–23, revised 1996. NIH, Bethesda, MD.

Quantock AJ, Kratz-Owens KL, Leonard DW, *et al.* 1994; Remodelling of the corneal stroma after lamellar keratoplasty: a synchrotron X-ray study. *Cornea* **13**: 20–27.

Robert L, Legeais JM, Robert AM. *et al.* 2001; Corneal collagens. *Pathol Biol (Paris)* **49**: 353–363.

Schwartz EC, Huss R, Hopkins A, *et al.* 1997; Blindness and visual impairment in a region endemic for onchocerciasis in the Central African Republic. *Br J Ophthalmol* **81**: 443–447.

Sharma A, Gupta P, Narang S, *et al.* 2001; Clear tectonic penetrating graft using glycerine-preserved donor cornea. *Eye (Lond)* **15**: 345–347.

Streilein JW, Yamada J, Dana MR, *et al.* 1999; Ksander BR. Anterior chamber-associated immune deviation, ocular immune privilege, and orthotopic corneal allografts. *Transplant Proc* **31**: 1472–1475.

Tanaka Y, Shi D, Kubota A, *et al.* 2011; Irreversible optical clearing of rabbit dermis for autogenic corneal stroma transplantation. *Biomaterials* **32**: 6764–6772.

Vijayasekaran S, Hicks CR, Chirila TV, *et al.* 1997; Histologic evaluation during healing of hydrogel core-and-skirt keratoprostheses in the rabbit eye. *Cornea* **16**: 352–359.

de Vries Reilingh TS, Bodegom ME, van Goor H, *et al.* 2007; Autologous tissue repair of large abdominal wall defects. *Br J Surg* **94**: 791–803.

Watanabe T, Kanda K, Yamanami M, *et al.* 2011; Long-term animal implantation study of biotube-autologous small-caliber vascular graft fabricated by in-body tissue architecture. *J Biomed Mater Res B Appl Biomater* **98**: 120–126.

Whitcher JP, Srinivasan M, Upadhyay MP. 2001; Corneal blindness: a global perspective. *Bull World Health Org* **79**: 214–221.

Whitcher JP, Srinivasan M, Upadhyay MP. 2002; Prevention of corneal ulceration in the developing world. *Int Ophthalmol Clin* **42**: 71–77.

Williams KA, Coster DJ. 2007; The immunobiology of corneal transplantation. *Transplantation* **84**: 806–813.

Xiao J, Duan H, Liu Z, *et al.* 2011; Construction of the recellularized corneal stroma using porous acellular corneal scaffold. *Biomaterials* **32**: 6962–6971.

Yamanami M, Yahata Y, Uechi M, *et al.* 2010; Development of a completely autologous valved conduit with the sinus of Valsalva using in-body tissue architecture technology: a pilot study in pulmonary valve replacement in a beagle model. *Circulation* **122**(11 Suppl): 100–106.

Yoeruek E, Bayyoud T, Maurus C, *et al.* 2011; Reconstruction of corneal stroma with decellularized porcine xenografts in a rabbit model. *Acta Ophthalmol* **90**: e206–e210.

Artificial
Organs

In Vitro Evaluation of a Novel Autologous Aortic Valve (Biovalve) With a Pulsatile Circulation Circuit

*Hirohito Sumikura, †Yasuhide Nakayama, *Kentaro Ohnuma, *Yoshiaki Takewa, and *Eisuke Tatsumi

*Departments of *Artificial Organs and †Biomedical Engineering, National Cerebral and Cardiovascular Center Research Institute, Suita, Osaka, Japan*

Abstract: We have used in-body tissue architecture technology to develop an autologous valved conduit with intact sinuses of Valsalva (biovalve). In this study, we fabricated three different forms of biovalves and evaluated their function in vitro using a mock circulation model to determine the optimal biovalve form for aortic valve replacement. A cylindrical mold for biovalve organization was placed in a dorsal subcutaneous pouch of a goat, and the implant that was encapsulated with connective tissue was extracted 2 months later. The cylindrical mold was removed to obtain the biovalve (16 mm inside diameter) that consisted of pure connective tissue. The biovalve was connected to a pulsatile mock circulation system in the aortic valve position. The function of the three biovalves (biovalve A: normal leaflets with the sinuses of Valsalva; biovalve B: extended leaflets with the sinuses of Valsalva; biovalve C: extended leaflets without the sinuses of Valsalva) was examined under pulsatile flow conditions using saline. In addition, the mock circuit was operated continuously for 40 days to evaluate the durability of biovalve C. The regurgitation rate (expressed as a percent of the mean aortic flow rate during diastole) was 46% for biovalve A but only 3% for biovalves B and C. The durability test demonstrated that even after biovalve C pulsated more than four million times (heart rate, 70 bpm; mean flow rate, 5.0 L/min; mean aortic pressure, 92 mm Hg), stable continuous operation was possible without excessive reduction of the flow rate or bursting. The developed biovalve demonstrated good function and durability in this initial in vitro study. **Key Words:** Heart valve—Biovalve—Pulsatile circulation circuit—Autologous tissue—Aortic valve—Tissue engineering.

Prosthetic valve replacement is an essential treatment for severe valvular heart disease (1). Mechanical valves and biological valves provide excellent valvular function and are currently implanted to treat serious valve disease. However, both of these valves have limitations. Although mechanical valves are durable, anticoagulants such as warfarin are required to prevent thrombosis. Although biological valves, which are usually heterologous (made of bovine pericardia or porcine valves), are less thrombogenic, they may undergo calcification and structural deterioration over time.

Recently, heart valve prostheses have been developed using tissue engineering technology, and advantages of these tissue-engineered valves would likely include nonthrombogenicity, infection resistance, and cellular viability. If tissue-engineered valves are implanted in children, there is the possibility of growth, repair, and remodeling as a child matures, thus eliminating the repetitive surgeries typically required to implant conventional mechanical or biological valves as body size increases (2). We have been developing autologous prosthetic tissues to function as heart valves or grafts using "in-body tissue architecture technology," which is a novel concept in regenerative medicine based on the tissue encapsulation phenomenon of foreign materials in living bodies (3–7). This technology involves the use of living bodies as reactors, and its advantages are that it is simple, safe, and cost-effective. In previous studies, we used this technology to develop an autologous valved conduit with the sinuses of Valsalva and named this new valve the "biovalve" (5–7). The biovalve was developed using a canine model , and its function was determined when it was

doi:10.1111/aor.12173

Received April 2013; revised July 2013.

Address correspondence and reprint requests to Dr. Hirohito Sumikura, National Cerebral and Cardiovascular Center Research Institute, Department of Artificial Organs, 5-7-1 Fujishirodai, Suita-Shi, Osaka 565-8565, Japan. E-mail: sumikura@ri.ncvc.go.jp

used to replace the pulmonary valve (5). Smooth opening and rapid closing of the leaflets were confirmed in vitro. In addition, the biovalve was implanted in beagles to replace the pulmonary valve and was able to maintain normal hemodynamic function for approximately 3 months. To further develop the biovalve, our goal is to fabricate the biovalve using large animals and to engineer a valve that can replace the aortic valve. Recently, biovalves were fabricated using goats and showed smooth movement of the leaflets with little regurgitation when they were implanted in a specially designed apico-aortic bypass circuit in a goat model (7). Further evaluation of valvular function and an endurance test is needed to determine the optimal form of the biovalve that should be used to replace the aortic valve.

In this study, we fabricated three different forms of biovalves and evaluated their function and durability using a mock circulation model in vitro.

MATERIALS AND METHODS

Preparation of biovalves

Figure 1 shows the process of preparation of the biovalves. A specially designed cylindrical mold for biovalve organization is shown in Fig. 1a. The cylindrical mold was constructed from seven plastic parts. First, three small hemisphere-like parts with projections resembling the protrusion of the sinuses of Valsalva were fastened between two tube-like parts (diameter, 16 mm) that served as the conduit, with a small aperture of 0.5 mm. Second, the combined parts were fixed with a rod-like center part and a latch part to obtain the final mold. The mold was designed such that the leaflets were separated from each other in the open form and connective tissue entered through its aperture (8). We chose goats as an experimental animal in order to evaluate the biovalve in an environment similar to the valve size and hemodynamics in humans. Several cylindrical molds were placed in a dorsal subcutaneous pouch in 10 goats (age, 1–2 years; body weight, 40–50 kg) under general anesthesia induced with 10 mg/kg of ketamine and maintained with 1–3% isoflurane (Fig. 1b). The implant which was encapsulated with connective tissue was extracted 2 months later (Fig. 1c). The cylindrical mold was removed from the implant to obtain the biovalve that consisted of pure connective tissue (Fig. 1d,e). The biovalve was stored at −30°C in 70% ethanol. As the storage in 70% ethanol is not fixation but dehydration of the tissue, the suppleness of the biovalves which were rehydrated recovers. The biovalve including the leaflets, conduit, and sinus of Valsalva was mainly composed of collagen-rich tissue with fibroblasts (Fig. 1f,g). There were few elastic fibers and vascular cells. The elongation at the break, indicative of tissue extensibility, was obtained from the stress-strain curves which were measured using a tensile tester (7). The elongation at the break in the leaflet and conduit of the biovalve were 66.7 ± 8.3 and 68.7 ± 6.9%. Here, the elongation at the break in the leaflet and conduit of the native valve were 108.3 ± 12.5 and 64.6 ± 10.4%. Although elongation at the break in the leaflet of the biovalve was about a

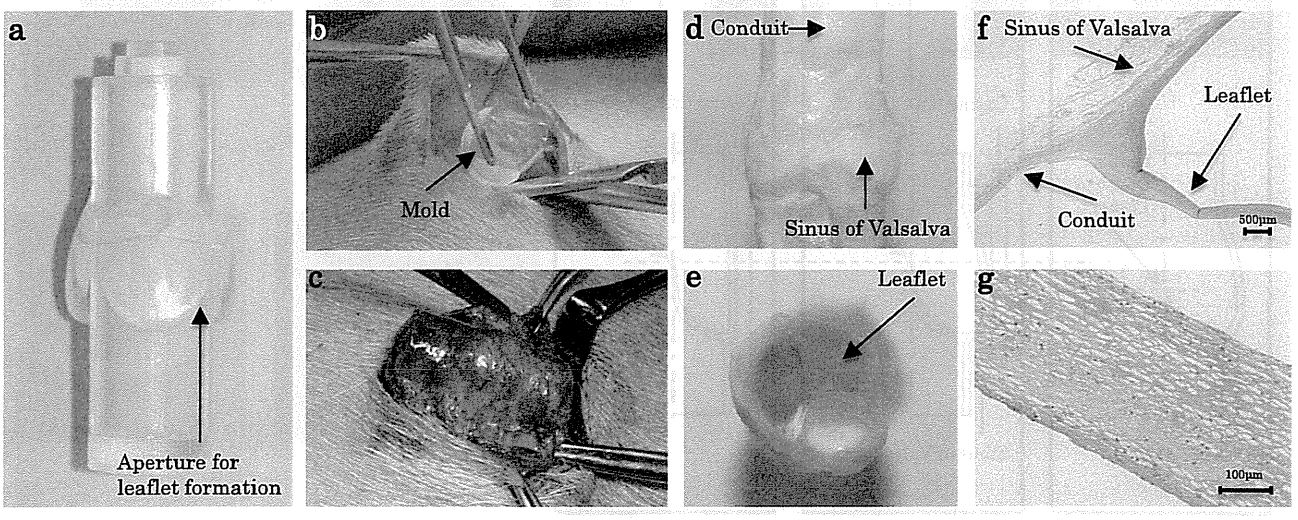

FIG. 1. Preparation process of the biovalve. (a) A specially designed cylindrical mold was constructed from seven plastic parts to act as a scaffold for the biovalves. (b) The mold was placed in the dorsal subcutaneous pouch of a goat. (c) The implant which was encapsulated with connective tissue was extracted 2 months later. (d, e) The cylinder mold was removed from the implant, and the biovalve completely produced only by connective tissue was obtained. (f) The cross section of the whole biovalve stained with hematoxylin and eosin. (g) The extended cross section of the leaflet stained with hematoxylin and eosin.

TABLE 1. *Biovalve measurements*

Outer diameter of conduit (mm)	17
Inner diameter of conduit (mm)	16
Maximum diameter at the sinuses of Valsalva (mm)	19
Tissue thickness (mm)	0.5
Length (mm)	55

half of the native value, the biovalve had suppleness similar to the native valve. Although these data were measured after storage in 70% ethanol, the suppleness of the biovalves was maintained. The dimensions of the biovalve are given in Table 1.

Institutional guidelines for the care and use of laboratory animals were observed. All protocols were reviewed and approved by the Animal Subjects Committee of the National Cerebral and Cardiovascular Center (no. 12002).

Valves evaluated

There were five different valves examined in this study (Fig. 2). Three of the valves were biovalves with slightly different designs (Fig. 2a–e), and two were commercially available valves that were compared with the biovalves. The latter two valves were a biological valve (19 mm, St. Paul, MN, USA) (Fig. 2f) and a mechanical valve (23 mm, Bicarbon Bileaflet Valve, Sorin Biomedica, Saluggia, Italy) (Fig. 2g).

Biovalve A (Fig. 2a) was developed with the sinuses of Valsalva using the same mold as in a previous study (8). The leaflets of this biovalve were designed to conform to the shape of a porcine valve. Each leaflet had an area of 240 mm^2 and a length of 17 mm (Fig. 2d).

Biovalve B (Fig. 2b) was fabricated with leaflets that were 2 mm longer in an axial direction than biovalve A. This was done to improve the operating performance of the biovalve under systemic circulatory conditions. This model also had an outer casing (19 mm inner diameter) that allowed growth of the sinuses of Valsalva in a radial direction. Each leaflet had an area of 290 mm^2 and a length of 19 mm (Fig. 2e).

Biovalve C (Fig. 2c) was the same as biovalve B but without the sinuses of Valsalva to determine whether or not the presence of these sinuses influenced

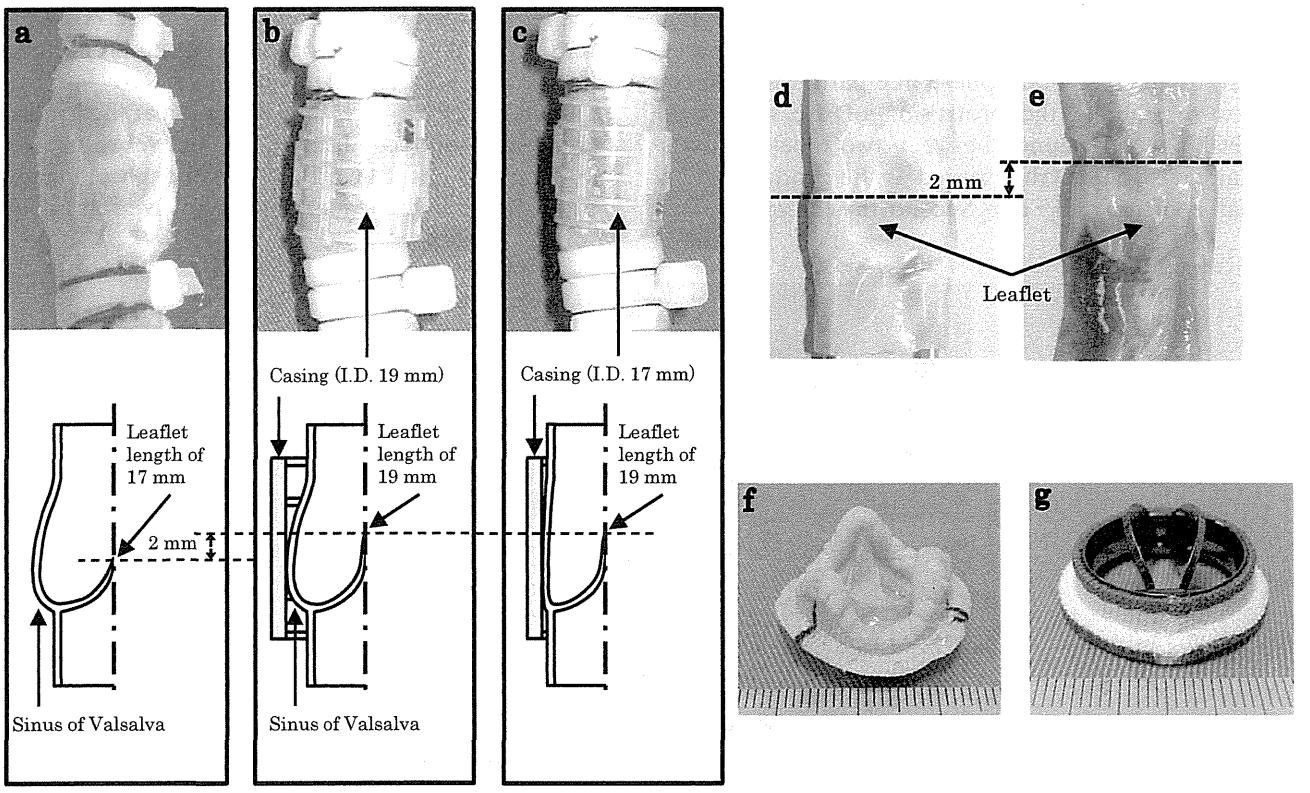

FIG. 2. The valves employed in this study. (a) Biovalve A had a leaflet length of 17 mm. (b) Biovalve B had a leaflet length of 19 mm and had an outside casing (19 mm inner diameter) that was used to prevent the sinuses of Valsalva from extending in a radial direction beyond the design value. (c) Biovalve C had a leaflet length of 19 mm and had an outside casing (17 mm inner diameter) that was used to prevent growth of the sinuses of Valsalva. (d) Interior surface of biovalve A. (e) Interior surface of biovalves B and C. (f) Biological valve (19 mm, Epic Supra Valve, St. Jude Medical, Inc.). (g) Mechanical valve (23 mm, Bicarbon Bileaflet Valve, Sorin Biomedica).